Journal of Hydrology 586 (2020) 124913

Contents lists available at ScienceDirect

Journal of Hydrology

journal homepage: www.elsevier.com/locate/jhydrol

Research papers

Multifractal description of daily rainfall fields over India

S. Adarsh[a], Vahid Nourani[b,c,*], D.S. Archana[d], Drisya S. Dharan[d]

[a] Department of Civil Engineering, TKM College of Engineering, Kollam 691005, Kerala, India
[b] Center of Excellence in Hydroinformatics, Faculty of Civil Engineering, University of Tabriz, Tabriz, Iran
[c] Faculty of Civil and Environmental Engineering, Near East University, Near East Boulevard, 99138, Nicosia, N. Cyprus, via Mersin 10, Turkey
[d] Department of Civil Engineering, TKM College of Engineering, Kollam 691005, Kerala, India

ARTICLE INFO

This manuscript was handled by C. Corradini, Editor-in-Chief, with the assistance of Renato Morbidelli, Associate Editor

Keywords:
Rainfall
Temperature
Multifractal
Correlation
Climate shift

ABSTRACT

This study investigated the scaling characteristics of daily rainfall time series over India and their spatio-temporal variability using Multifractal Detrended Fluctuation Analysis (MF-DFA) method. In the study, fine resolution gridded (1°x1°) dataset of daily rainfall for the period 1951–2016 was used for the analysis. The scaling characterization using MF-DFA shows that rainfall data of most of the grid points (over 87%) display short term persistence. The analysis of spatial variability of multifractal characteristics shows that the multifractal strength is strongest in the western and central India while the strength is the lowest in the north east region. Further, the evaluation of multifractal properties of rainfall time series of pre and post 1976/77 period of Pacific climate shift shows that there is a clear reduction in the multifractal strength and complexity for the post 1976/77 with contrasting behavior for the persistence. Finally, the association of daily rainfall with mean, maximum, minimum temperature values and the diurnal temperature range (DTR) time series of the 1951–2016 period were investigated using Multifractal Detrended Cross Correlation analysis (MF-DCCA). The nature and strength of association between the two variables of rainfall and temperature differs with time scales and it was found that the joint persistence of these variables lies between individual persistence property. There is a distinct difference in the persistence cross-correlation properties at the Peninsular region and coastal belts when compared with other regions in India and the difference is most perceptible in the T_{min}-rainfall link.

1. Introduction

The estimation of local fluctuations of hydrologic time series is one of the challenging problems in hydrologic time series analysis. In 1970s, the researchers identified fractal behavior of time series which is the property of a fragmental geometrical object that can be subdivided into parts each of which is a reduced size copy of the whole (Mandelbrot, 1982). Over the years, a large number of methods evolved for estimation of fractality of time series data. They include, double trace moments (Tessier et al., 1996), Fourier spectral analysis (Hurst, 1965; Pandey et al., 1998), extended self similarity (ESS) principles (Dahlstedt and Jensen 2005), wavelet transform modulus maxima (WTMM) (Kantelhardt et al., 2003), arbitrary order Hilbert spectral analysis (AOHSA) (Huang et al., 2009; Adarsh et al., 2018). Peng et al., (1994) proposed an efficient method namely Detrended Fluctuation Analysis (DFA) to perform the fractal analysis based on a detrending procedure. Kantelhardt et al., (2002) proposed the multifractal extension of DFA procedure, popularly known as multifractal DFA (MF-DFA). For hydrological time series, the multifractal description can be regarded as a 'fingerprint' of the time series and it serves as an efficient nontrivial test bed for the performance of state-of-the-art rainfall-runoff models (Kantelhardt et al., 2006).

Description of multifractal behavior of daily rainfall fields was one of the major domains of research among hydrologists in the past two decades and the researchers used a multitude of techniques for such analysis (Olsson and Niemczynowicz, 1996; Tessier et al., 1996; Kantelhardt et al., 2003; Yu et al., 2014; Krzyszczak et al., 2018; Garcia-Marin et al., 2019). In one seminal work by Kantelhardt et al., (2006), the authors investigated the multifractal behavior of 99 long term daily precipitation records and 42 long term daily runoff records from different parts of the world. They found that the precipitation generally shows short term persistence and runoff time series show long term persistence with a mean scaling exponent of ~0.73 for runoff and ~0.53 for precipitation records. The development of MF-DFA method was a major breakthrough in the multifractal characterization of rainfall fields (Yu et al., 2014; Tan and Gan 2017; Krzyszczak et al., 2018). Even though several studies performed fractal analysis employing MF-DFA procedure worldwide, according to the authors' knowledge, no

* Corresponding author at: University of Tabriz, 29 Bahman Ave., Tabriz 5166616471, Iran.
E-mail address: nourani@tabrizu.ac.ir (V. Nourani).

https://doi.org/10.1016/j.jhydrol.2020.124913
Received 15 January 2020; Received in revised form 14 March 2020; Accepted 30 March 2020
Available online 01 April 2020

comprehensive study on the multifractality of rainfall time series of India and the spatio-temporal variability of the multifractal parameters are reported. Rainfall is a complex phenomenon gets resulted from the favorable conditions of a large number of meteorological variables like temperature, humidity, wind velocity and large scale circulations. Being a multiscale process, understanding the teleconnections of rainfall with such variables in different time scales will be giving better insights to the associated physical processes (Adarsh and Janga, 2016). Multifractal theory is a useful alternative to investigate such teleconnections of non-stationary time series in multiple time scales. Detrended cross-correlation analysis (DCCA), proposed by Podobnik and Stanley (2008) was one of the initial attempts to investigate cross correlations between two dependent time-series signals of non-stationary characteristics. Its multifractal extension namely MF-DCCA proposed by Zhou (2008), which involves a procedure quite similar to the MF-DFA algorithm, except for the capability to handle two candidate series simultaneously. The method could gain wide popularity in the analysis of hydro-meteorological time series (e.g., Hajian and Movahed 2010; Wu et al., 2018; Dey and Mujumdar 2018). However, so far no study reported the rainfall-temperature cross correlations in a multifractal framework.

In view of the above review, the specific objectives of this paper can be stated as: (i) to determine multiftactal properties of daily gridded rainfall data of India and to investigate their spatio-temporal changes; (ii) to investigate the cross-correlation between rainfall and four temperature time series (minimum, maximum, mean and diurnal temperature range (DTR)) using the MF-DCCA method. In section 2, the overall framework followed and algorithms of methodologies used in the study are described. In section 3, the details of study area and data are presented. In section 4, the results supporting the stated objectives of the study are presented. Section 5 presents the possible applications and scope for future studies and in the final section, important conclusions of the study are presented.

2. Materials and methods

This study firstly provides a generalized framework which can be followed for multifractal analysis of any two correlated time series. The potential of MF-DFA can be used for the detection of multifractality of the time series of concern and the information on scaling behaviour and the parameters obtained may eventually help for performing multifractal modelling (Cadenas et al., 2019). Apart from the above, analysing the spatio-temporal variability of the prominent multifractal parameters may help in capturing the significant changes in persistence or multifractal properties over different time spells, which in-turn may infer non-stationarity of the time series. Subsequently, non-stationarity modelling approaches can be followed to get promising results against the modelling with stationarity assumptions. The detection of multifractality will help to investigate the mutual association between two correlated time series in multiple time scales in a multifractal perspective using robust methods like MF-DCCA. The procedure followed in this study involves the conjunctive use of two popular and widely accepted methods like MFDFA and MF-DCCA for getting improved understanding of the rainfall characteristics of Indian subcontinent and for getting new insights into the rainfall-temperature cross correlations. In short, the methodology followed is a general one, the algorithms used are well accepted by the scientific community and it can be applied for any complex time series datasets irrespective of the regional differences. The flowchart of the procedure followed is presented in Fig. 1 and the details of the MF-DFA and MF-DCCA are provided in subsequent sections.

2.1. Multifractal detrended Fluctuation analysis (MF-DFA)

MF-DFA is a popular mathematical tool for detection of the scaling characteristics and multifractality of time series datasets. The steps of MF-DFA algorithm can be presented as given below (Kantelhardt et al., 2002; Li et al., 2015; Adarsh et al., 2019):

(i) For a time series X (x_1, x_2… x_N), determine the cumulative deviation of the time series known as its 'profile'

$$P(i) = \sum_{k=1}^{i} [x_k - \bar{x}] \tag{1}$$

where $i = 1, 2, \ldots\ldots, N$, $\bar{x}$ and N are the mean and length of the time series,

(ii) Subdivide the profile $P(i)$ into $N_s = \mathrm{int}(N/s)$ non-overlapping segments of length 's', which is the segment sample size (popularly called as scale) and int() refers the integer part. As N needs not to be an integer multiple of s, to avoid the possible exclusion of data points from the tail end of the series, the division needs to be performed starting from the tail end also, which will lead to a total of $2N_s$ segments in the calculations,

(iii) Estimate the local trend for each of the $2N_s$ segments by the method of least squares (Kantelhardt et al., 2006)

$$F^2(s, \nu) = \frac{1}{s} \sum_{i=1}^{s} \{P[(\nu - 1)s + i] - p_\nu(i)\}^2 \; for \; \upsilon = 1, 2, \ldots\ldots, N_s \tag{2}$$

and

$$F^2(s, \nu) = \frac{1}{s} \sum_{i=1}^{s} \{P[N - (\nu - N_s)s + i] - p_\nu(i)\}^2 \; for \; \upsilon = N_s + 1, \ldots\ldots, 2N_s \tag{3}$$

Here $p_\upsilon(i)$ is the fitting polynomial of any appropriate order in segment υ,

(iv) Find out the fluctuation function (FF) for any generic statistical moment order q as follows:

$$F_q(s) = \left\{ \frac{1}{2N_s} \sum_{\nu=1}^{2N_s} [F^2(s, \nu)]^{q/2} \right\}^{1/q} \tag{4}$$

Here, any real value except zero can be assigned to the moment order q.

For the zeroth moment order, FF can be computed by a logarithmic averaging procedure as given below (Kantelhardt et al., 2002):

$$F_0(s) = \exp\left\{ \frac{1}{4N_s} \sum_{\nu=1}^{2Ns} \ln[F^2(s, \nu)] \right\} \tag{5}$$

(v) Determine the scaling characteristics of the FFs for different moment orders, by analysing the logarithmic plots of $F_q(s)$ versus s. $F_q(s)$ bears the relation $F_q(s) = s^{h(q)}$, if the time series is power-law correlated. The power $h(q)$ is designated as generalized Hurst exponent (GHE). For stationary time series, $0 < h(q = 2)$ less than 1, is identical to the classical Hurst exponent (H). If $0.5 < H \leqslant 1$, the time series possess long term persistence (long memory); if $0 \leqslant H < 0.5$, the time series possess short term persistence (short memory) and if $H = 0.5$, the time series is uncorrelated. Long term persistence implies a positive auto correlation in the time series (i.e., the effect of an observation on future observations remains significant for a long period of time). The selection of scale (s) range, the type of polynomial chosen etc. are some of the key issues while applying the MF-DFA method. Their appropriate selection involves a trial and error procedure and some thumb rules can be found in literature (Ihlen 2012; Wang et al. 2016).

The Hurst exponent ($h(q = 2)$) basically helps to comment on persistence of the time series while the derived exponents such as q-order mass exponent ($\tau(q)$) and singularity exponent (α) helps to comment on the multifractality of the time series. These exponents can be mathematically calculated as (Li et al., 2015):

$$\tau(q) = qh(q) - 1 \tag{6}$$

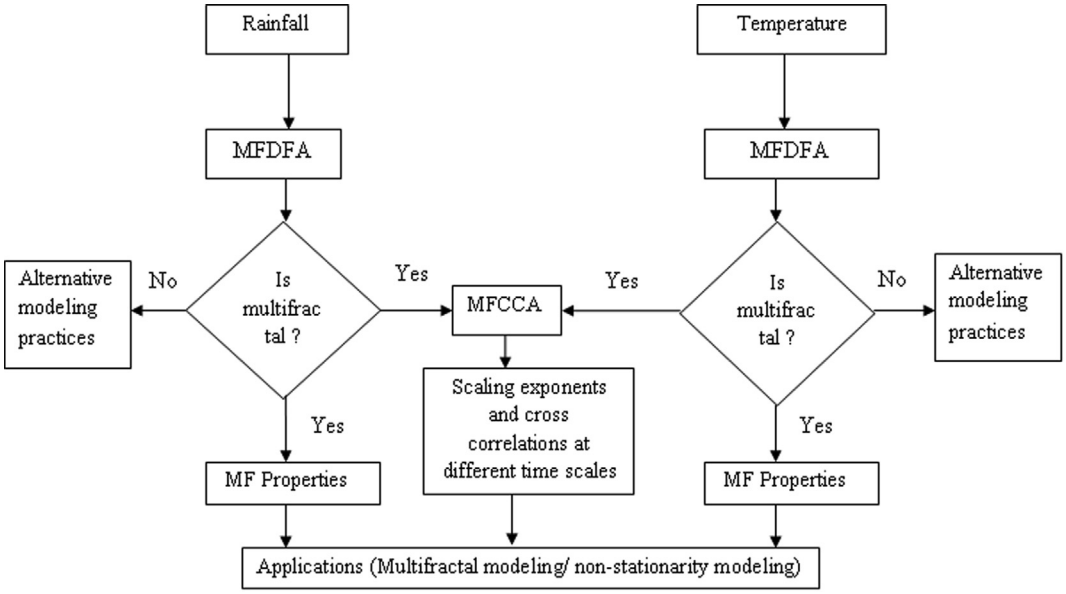

Fig. 1. Methodology of multifractal analysis of rainfall and temperature data.

$$\alpha = \frac{d\tau(q)}{dq} \tag{7}$$

and

$$f(\alpha) = q\alpha - \tau(q) \tag{8}$$

Where the plot of $f(\alpha)$ vs α is called as the singularity spectrum. The base width of the spectrum ($\Delta\alpha = \alpha_{max} - \alpha_{min}$) depicts the degree of multifractality (DoMF) of the time series. A wider singularity spectrum indicates a higher DoMF and vice versa. If the time series is multifractal, the singularity spectrum will be an inverted parabola. Asymmetry Index (R) is another useful parameter for multifractal analysis derived from the shape of the multifractal spectrum (Drożdż and Oświecimka, 2015):

$$R = \frac{\Delta\alpha_{left} - \Delta\alpha_{right}}{\Delta\alpha_{left} + \Delta\alpha_{right}} \tag{9}$$

where $\Delta\alpha_{left} = \alpha_0 - \alpha_{min}$ and $\Delta\alpha_{right} = \alpha_{max} - \alpha_0$are respectively, the width of left- and right-hand wings of the multifractal spectrum; their values describe the distribution patterns of high and low fluctuations andα_0 is the singularity exponent (known as Holder exponent) for $q = 0$. R ranges from -1 to 1. $R = 0$ represents a symmetrical multifractal spectrum; $R > 0$ suggests a left-hand deviation of the multifractal spectrum, resulted from the time series with local high fluctuations; R less than 0 suggests a right hand deviation with local low fluctuations.

2.2. Multifractal detrended cross correlation analysis (MF-DCCA)

In order to quantify the inter-relationships between different hydrometeorological variables, different statistical measures are used out of which most popular and simplest one is the Pearson correlation coefficient. However, the robustness of this coefficient is debatable in the presence of outliers and if the data is of non-linear and non-stationarity in character (Piao and Fu 2016). For the real field data (which often possess non-linear and non-stationarity characteristics) spurious correlation may be reported as they always characterized by trend. Because of this, an estimation measure supported by the detrending operation such as MF-DCCA is advisable. The different steps involved in MF-DCCA computational procedure can be described as follows:

(i) For two time series x_i of y_i and ($i = 1,2,\ldots,N$); determine the profiles as :

$$X(k) = \sum_{k=1}^{i} [x_k - \bar{x}] \tag{10}$$

$$Y(k) = \sum_{k=1}^{i} [y_k - \bar{y}] \tag{11}$$

where, $i = 1,\ldots\ldots, N$; and $\bar{x}$and $\bar{y}$are the means of two time series,

(ii). Divide $X(k)$ and $Y(k)$into N_s non overlapping segments, thus $2N_s$ segments are obtained,

(iii). Calculate the local trend of $X(k)$ and $Y(k)$ for each of $2N_s$ segments, and determine the covariance:

$$f^2_{DCCA}(s, i) = \left\{ \frac{1}{s} \sum_{k=i}^{i+n} [((x_k - \bar{x})((y_k - \bar{y})] \right\} \tag{12}$$

(iv). Calculate detrended covariance by summing over all overlapping segments of length as:

$$F(s) = \left\{ \frac{1}{2N_s} \sum_{i=1}^{2N_s} [f^2_{DCCA}(s, i)] \right\}^{1/2} \tag{13}$$

$F(s)$ behaves as a power-law function of s (the scaling behavior), where s is the segmental sample size as $F(s) \sim s^{\lambda(q)}$. The cross-correlation exponent $\lambda(q)$, designed as scaling exponent, can be obtained by deriving the slope of log–log plot of $F(s)$ versus s by the method of least squares.

Cross-correlation coefficient is defined as the ratio between the detrended covariance function F_{DCCAxy} and the detrended variance functions $F_{DFAx}$and F_{DFAy}as (Zebende 2011; Vassoler and Zebende 2012; Oświecimka et al., 2014; Kwapień et al., 2015) :

$$\rho_{DCCA} = \frac{F_{DCCAxy}}{F_{DFAx}. F_{DFAy}} \tag{14}$$

Theoretically, the value of ρ_{DCCA} ranges as $-1 \leq \rho_{DCCA} \leq 1$. The values range between $\pm$ 0.666 to $\pm$ 1 , $\pm$ 0.333 to $\pm$ 0.666, $\pm$ 0 to $\pm$ 0.333 show respectively strong positive (negative), medium and weak cross correlations (Brito et al., 2018).

3. Study area and database

The daily gridded rainfall time series at 1°x1° resolution (one-time series over each cell) for the period 1951–2016 received from India

Table 1
Descriptive statistics of rainfall values of daily gridded data.

Property	Range
Maximum (mm)	69.5–874
Mean (mm)	0.565–11.51
Standard deviation	3.52 – 26.5
Zero values	10520–22037
% Zero values	44.31–92.82

Meteorological Department (IMD) were used in the present study. A total of 286 grid points where long and continuous data were available and identified for performing the analysis. Brief statistics of the rainfall of different grid points are given in Table 1.

The spatial variability of multifractality was investigated by considering five rainfall homogeneous regions in India. The non-overlapping rainfall homogeneous regions have been defined by Indian Institute of Tropical Meteorology (IITM) Pune. The five regions include North West India (NWI), South Peninsular India (SPI), North East India (NEI), Central North East India (CNEI) and Western Central India (WCI). These regions are defined by rainfall homogeneity, by grouping the different meteorological subdivisions. The map showing rainfall homogeneous regions in India is presented in Fig. 2.

For investigating the cross correlation of rainfall with temperature time series, 1^{o}x1^{o} gridded extreme temperature (T_{max} and T_{min}), mean temperature (T_{mean}) and diurnal temperature range ($T_{DTR,}$ which is the difference between maximum and minimum temperature values) datasets at the same period (1951–2016) were used in this study.

4. Results and discussion

This section first presents the results of MFDF analysis of daily rainfall time series of different grid points along with the spatial variability. To examine the temporal change in multifractal properties of rainfall, the time series was partitioned into two periods with respect to the well recognized global climatic shift of 1976/77 and the results of MF analysis of the pre and post 1976/77 periods are presented here. Subsequently, the results of MF-DCCA between four different pairs of temperature-rainfall time series are presented.

4.1. Spatial variability of multifractal properties of rainfall

The MFDF analysis of daily gridded rainfall data for 1951 to 2016 was performed by considering a moment order of −4 to 4 (Drożdż et al., 2019). It should be noted that long and consecutive zero values are present in each grid points and with percentage varies between 44 and 92, in different grids (Table 1). This needs special attention while performing MF-DFA analysis, to avoid any possible conclusions on long term persistency in the datasets, which may be a spurious and erroneous interpretation. To avoid any possible bias or misinterpretations because of the long and consecutive zero values in the records, the minimum scale was chosen greater than the longest stretch of consecutive zero values in each time series (Drożdż et al., 2019). Different multifractal parameters like Hurst exponent, the spread of Generalized Hurst exponent plot ($\Delta h(q)$), spectral width, Holder exponent (α_0), asymmetry index (R), difference between singularity spectrum plot ($\Delta f(\alpha)$) etc were determined for all identified 286 grid points over India. The spatial distributions of different multifractal parameters of rainfall data are presented in Fig. 3. The PDF and CDF of the parameters were estimated using the non-parametric kernel density estimator and presented in Fig. 4.

Fig. 3 shows that the persistence and multifractal behavior of rainfall data is evident in gridded rainfall data of India. In most of the grid points (over 87%), the Hurst Exponent (H) values are less than 0.5 (indicating short term persistency). The mean value of Hurst exponent was found to be 0.385, which is also in line with the short term persistency of rainfall records of different parts of the globe reported earlier (Kantelhardt et al., 2006; Yu et al., 2014). To evaluate the degree of multifractality, $\Delta h(q)$ values were estimated. Higher value of $\Delta h(q)$ indicates a steeper GHE plot, in which variability in the distribution of high and low fluctuations is increased and the time series will be more complex and heterogeneous (Hou et al., 2018). Similar inference can also be made from the values of spectral width; the higher values of spectral width infer the high degree of multifractality. The mean value of $\Delta h(q)$ spectral width was found to be 0.498 and 0.873. In about 55% of the grid points, the value of $\Delta h(q)$ was found to be less than 0.5. The spectral width of majority of the points (about 74%) lies in the range 0.5 to 1. This may be because the rainfall process in India is highly intermittent and the time series of rainfall contains long and continuous zero values. About 94% of rainfall data have positive asymmetry index (R) value, which suggests left hand deviation with local low fluctuations. The negative value of asymmetry index was noted in the hilly terrains of northern India and few localized grids. The value of Holder exponent (α_0) indicates the complexity of the time series, and in this study the mean value of Holder exponent was found to be 0.44. Interestingly, the values of Holder exponent and Hurst exponent were well correlated with correlation value of 0.968. This is in agreement with the association between the two parameters reported by Burgueño et al., (2014) for the temperature time series. The difference between maximum and minimum values of singularity ($\Delta f(\alpha)$) provides an estimate of the spread in changes in fractal patterns. Since $\Delta f(\alpha)$ denotes the frequency ratio of the largest to the smallest fluctuations, a positive value of $\Delta f(\alpha)$ means that the largest fluctuations are more frequent than smallest fluctuations. The $\Delta f(\alpha)$ value was positive in most of the regions and a negative value of $\Delta f(\alpha)$ was noted only in the hilly terrains of the north and north-eastern parts of India.

Also to get an insight into multifractal property of rainfall data of different geographical regions, the rainfall time series of all grid points were segregated into that of five rainfall homogeneous regions. A total of 60, 67, 50, 69 and 40 grid points were identified respectively for the five rainfall homogeneous regions NWI, CNEI, NEI, WCI and PI. The multifractal properties estimated by the MF-DFA method were clustered into five groups and the PDFs and CDFs of different parameters were developed and presented in Fig. 5. The statistical properties of prominent multifractal parameters (Hurst exponent, spectral width and Holder exponent are presented in Table 2)

From Fig. 5, it is clear that the values and variability of Hurst exponent and spectral width are high in the North West India (NWI). It is well evident that the rainfall magnitude in regions like Rajasthan located in NWI India is so small and pattern is more predictable and homogeneous when compared to many of other regions of India. Also, higher persistence is noted in the rainfall of NEI region, which receives higher amount of rainfall within a typical year. The behavior of spread of GHE plot is in line with that of spectral width. The values of Holder exponent (α_0) (which is indicative of data complexity), is the highest in the NWI region and in the CNEI also, the rainfall pattern is complex in character. No specific pattern could be noted from the asymmetry index and $\Delta f(\alpha)$ of the rainfall data of different regions. From Table 2, it is noted that highest mean multifractal degree is noted in NWI and CNEI and overall variability in multifractal degree is the highest in NEI. On considering All India (AI), the variability in spectral width is considerably low than that of complexity and Hurst exponent. It is further noted that the variability of the persistence is the lowest at PI and NWI.

In order to verify the universality of this relationship, least square fit was made between Hurst exponent and Holder exponent, for All India (AI) and the five homogeneous regions and scatter plots of the same are presented in Fig. 6. Further, the correlations between the two exponents are found to be 0.98, 0.987, 0.979, 0.986 and 0.986 respectively for NWI, CNEI, NEI, WCI and PI. The high value of correlation confirms the universal property in the association between two multifractal exponents of rainfall datasets of geographical locations of India.

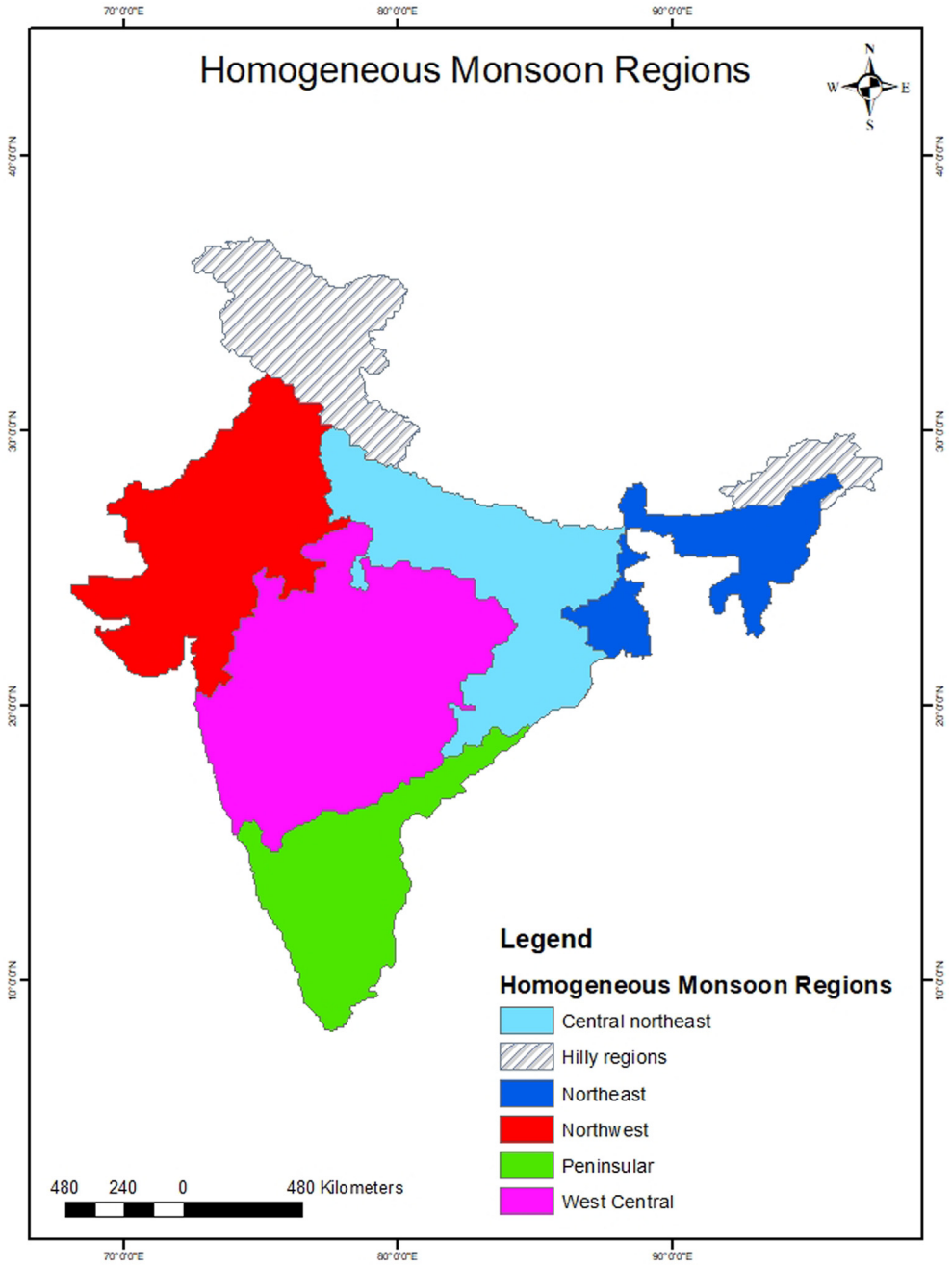

Fig. 2. Five rainfall homogeneous regions of India.

4.2. Temporal variability of multifractal properties of rainfall

To evaluate the temporal variability of the multifractal properties of rainfall, the time series of each grid point were partitioned into two sub-series with respect to the much debated Pacific climate shift of 1976/77 (Miller et al., 1994). It is well evident that the climatic shift influenced the pattern of Indian summer monsoon considerably (Sahana et al., 2015). The MFDFA was performed for the pre and post 1976/77 periods. The PDFs and CDFs of different multifractal parameters of rainfall time series for pre and post 1977 Pacific climatic shift are presented in Fig. 7.

From Fig. 7, it is clear that the multifractality and persistenace heve been affected by the climate shift of 1977. It is evident that there is a clear decrease in spectral width for rainfall after 1977, indicating the decrease in multifractality, while the persistence (indicated by Hurst exponent) and the complexity (indicated by the Holder exponent) have increased after this shift. On quantifying this change, it is noticed that 104 grid points showed a reduction persistance, none of the grid points displayed a swithover from short term to long term, while only three grids showed a swithover from long term to short term. The complexity of 132 grids and spectral width of 174 (61% grids) grid points displayed a reduction. The mean Hurst exponnet was 0.351 and spectral width of 0.82 for the pre 1977 period, while it was found to be 0.382 and 0.751 after the shift. There was a marginal difference in the mean of the complexity (0.43 and 0.446 for the pre and post 1977 periods respectively). The change in multifractal properties could also be connected with the change of the different multifractal properties of standardized precipitataion index (SPI) time series of post 1976/77 period computed based on spatially averaged rainfall dataset (Adarsh et al., 2019). But there is no such clear and consistent reduction in asymmetry index of rainfall time series of different grid points. In certain grid points, the spectral assymetry was changed from positive to negative and vice

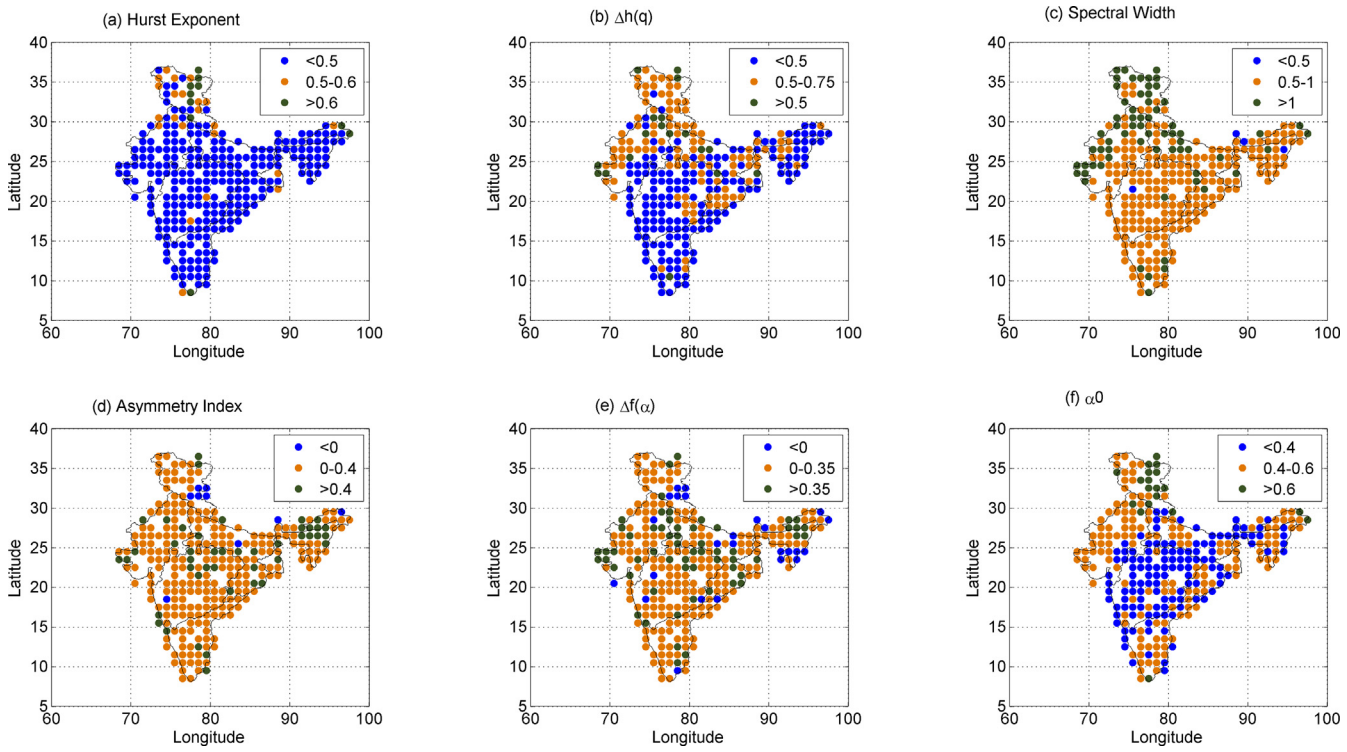

Fig. 3. Spatial distributions of multifractal parameters of rainfall data (a) Hurst exponent; (b) spread of generalized Hurst exponent (Δh(q)); spectral width; (d) asymmetry index (R); (e) spread of singularity spectrum (Δf(α)); (f) Holder exponent (α0).

versa in certain other grid points. i.e., there is no consistent increase or decrease in extremes at different grid points, but it displays spatial diversity. To investigate the change in multifractal properties, the four temperature time series were analysed by partitianing the data and the results are presented in Fig. 8.

The behaviour of temperature time series was quite contrasting to that of rainfall, as for temperature also there is a clear reduction in persistence and multifractality after the climate shift of 1977. The

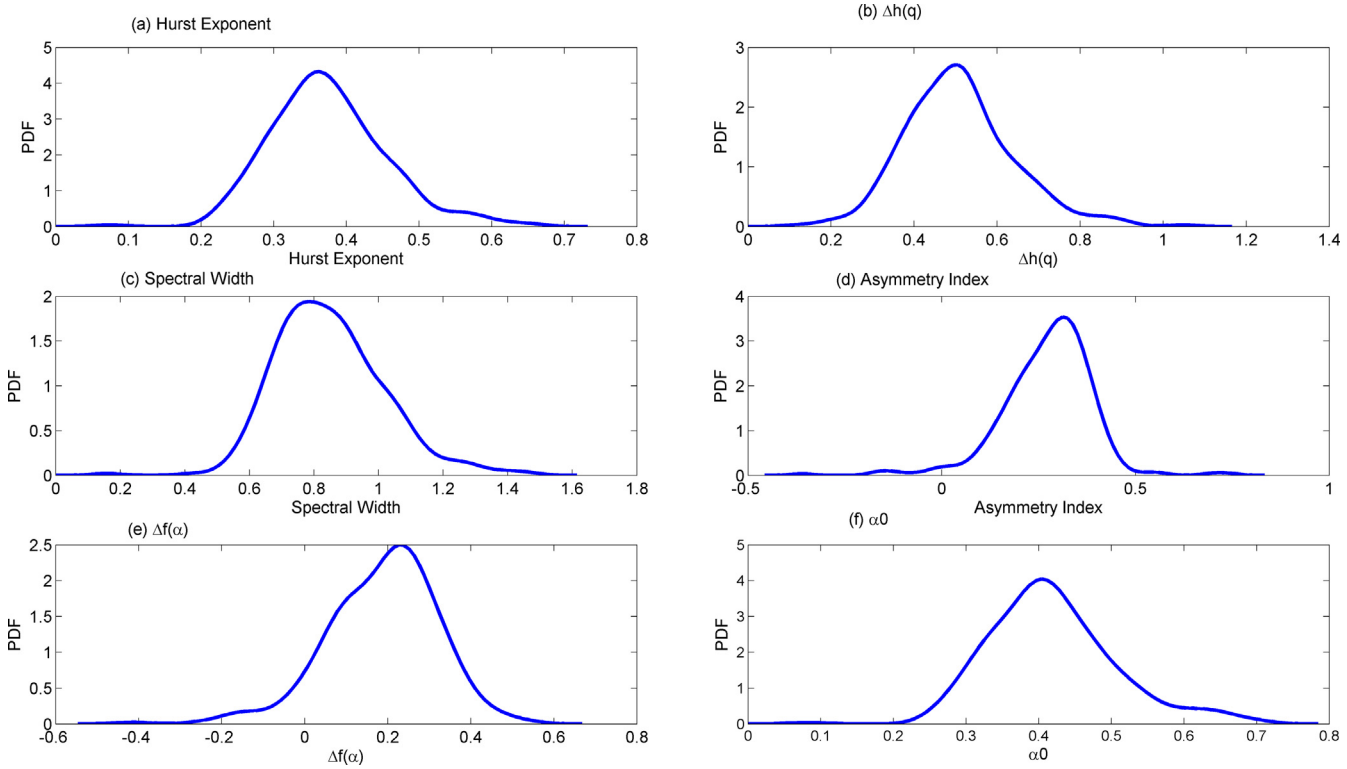

Fig. 4. PDFs of different multifractal parameters of rainfall data (a) Hurst exponent; (b) spread of generalized Hurst exponent (Δh(q)); spectral width; (d) asymmetry index (R); (e) spread of singularity spectrum (Δf(α)); (f) Holder exponent (α0).

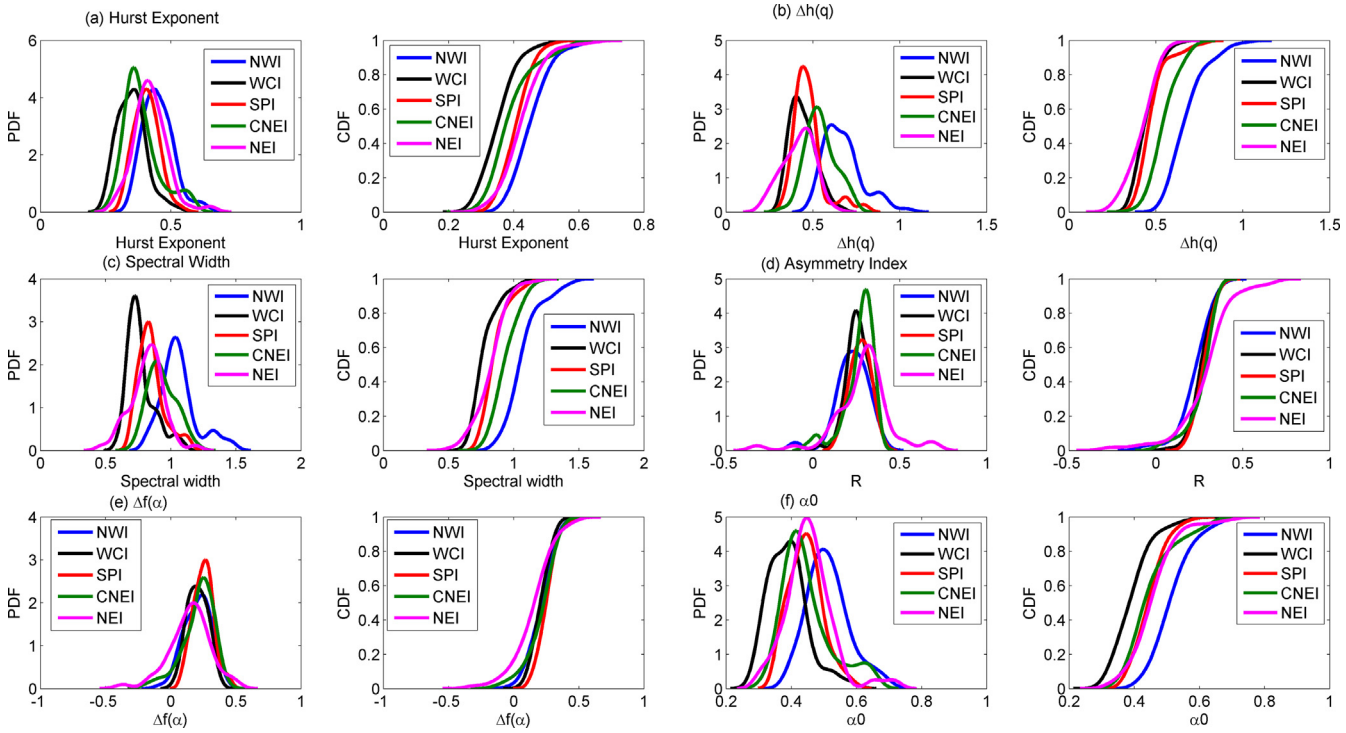

Fig. 5. PDFs and CDFs of different multifractal properties of rainfall data over different rainfall homogeneous regions (a) Hurst exponent; (b) spread of generalized Hurst exponent (Δh(q)); spectral width; (d) asymmetry index (R); (e) spread of singularity spectrum (Δf(α)); (f) Holder exponent (α0).

increased urbanization might have a key role and it might have weakened the multifractality of the temperature time series by creating more irregular profiles and smoothening the time series (Karatasou and Santamouris 2018) which in turn have severe influence on the multifractality of rainfall time series in the recent years.

The multifractal properties of rainfall could be linked with the physical mechanisms leading to the rainfall. Apart from the global parameters like terrestrial radiations and temperature, the local factors like the latitude, oceanic and atmospheric circulations, topography and local processes may influence the multifractality of the rainfall time series. The rainfall of India is highly intermittent in character which leads to high degree of multifractality. Also, one cannot ignore the inextricable link between the precipitation and temperature of the region in the non-linear multifractal character of these time series and such links in the multifractality were analyzed in this study using the detrended cross-correlation analysis.

4.3. MF-DCCA between rainfall and temperature time series

The most readily and directly available meteorological variable influencing the rainfall process of the country is the temperature. The temperature extremes and the diurnal temperature range have remarkable roles in rainfall process of India (Vinnarasi et al., 2017; Ross et al., 2018). In this study, the cross correlation between four temperature datasets of T_{max}, T_{mean}, T_{DTR} and T_{min} with rainfall were evaluated using the MF-DCCA method, considering the maximum scale as complete length of the time series in order to avoid any possible inconsistency in estimation of the scaling exponents. In order to get the reliable interpretations, because of long and continuous zero values in the records, the minimum scale was chosen much shorter than the longest stretch of consecutive zero values while performing the MF-DCCA. Figs. 9–12 show the spatial distribution of scaling exponent and different correlation coefficients obtained by the DCCA of rainfall and temperature time series. The correlation coefficients at two spatial scales corresponding to 90 days (termed as seasonal cross correlation) and those corresponding to 365 days (termed as annual cross correlation) along with overall correlation were considered in this analysis. Similarly, the individual scaling exponents of each variable along with the joint exponent were estimated for elucidating the persistence in different time series.

From the DCC analysis of T_{max}-rainfall link, it is noted that the scaling exponent of rainfall varies between 0.54 and 0.74 and that of maximum temperature varies between 0.8 and 0.99 and in all cases, λ value of temperature is more than that of rainfall. There is a dominancy of medium persistence (0.601–0.663) in the rainfall time series and such grid points are distributed in West Central, CNEI and NWI. The persistence values are relatively lower in the Peninsular India, even though all λ values are showing long term persistence. Very high and

Table 2
Statistical properties of prominent multifractal parameters of rainfall time series of All India and the homogeneous regions.

Region	Hurst exponent			Spectral width			Holder exponent		
	Mean	SD	CV (%)	Mean	SD	CV (%)	Mean	SD	CV (%)
AI	0.378	0.183	48.29	0.490	0.099	20.13	0.427	0.213	50.04
NWI	0.430	0.088	20.56	0.622	0.166	26.72	0.497	0.099	19.96
CNEI	0.372	0.103	27.77	0.551	0.131	23.81	0.429	0.113	26.38
NEI	0.400	0.093	23.29	0.409	0.151	36.74	0.434	0.099	22.72
WCI	0.321	0.085	26.51	0.409	0.113	27.70	0.360	0.089	24.85
PI	0.384	0.078	20.51	0.432	0.127	29.33	0.424	0.082	19.44

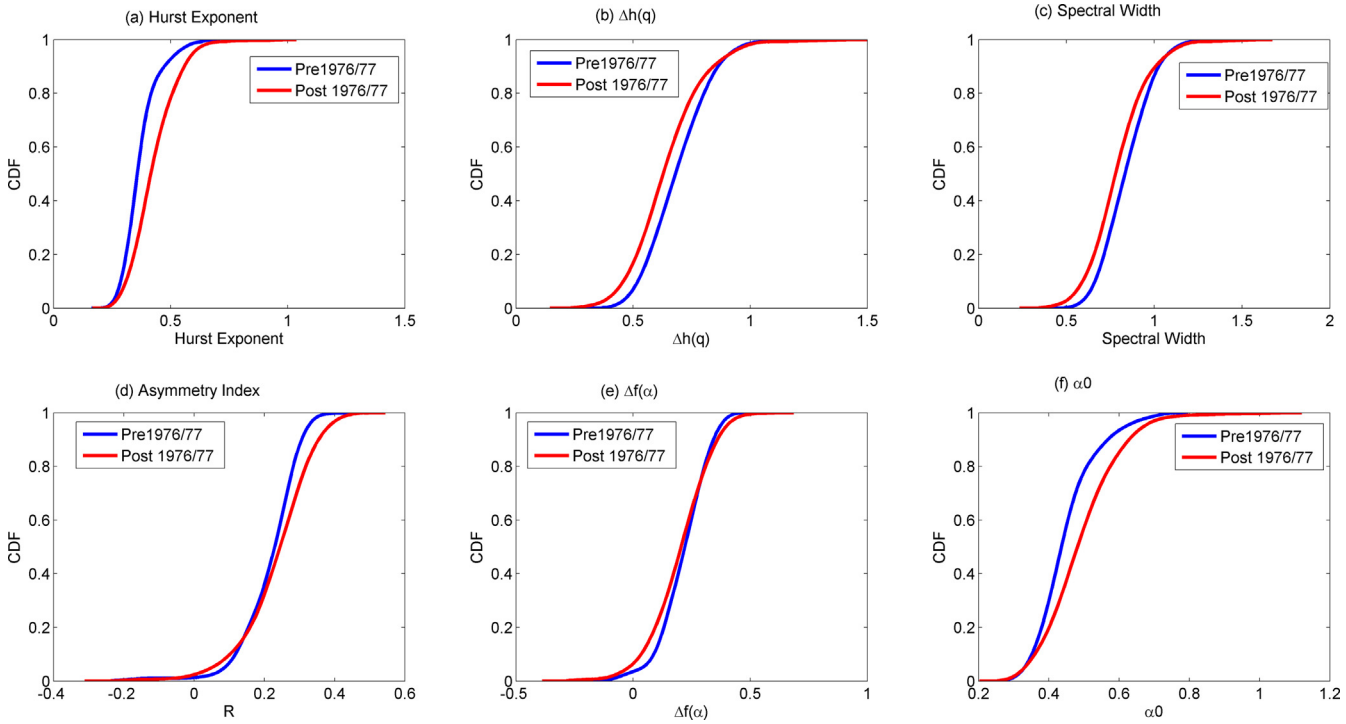

Fig. 6. PDF and CDF of multifractal properties of rainfall time series for pre and post 1977 Pacific climatic shift.

very low persistence of T_{max} time series are noticed in the eastern coast and north western regions, respectively.

At all grid points, the value of joint scaling exponent is nearly half of the scaling exponent of individual time series. i.e., the joint persistence is in between the individual persistence of the candidate variables (rainfall and temperature). This is in agreement with the universal property proven by the researchers considering the sunspot-streamflow linkages (Hajian and Movahed 2010). Except in the Peninsular India and western coast, the seasonal correlation is negative. But at annual scale, the negative correlation is displayed in the NWI and some parts of CNEI and WCI. In the Peninsular region and coastal belts of India in particular, the rainfall-T_{max} correlation is positive with relatively larger magnitude. The influence of large scale climatic oscillations from Indian Ocean (such as Equatorial Indian Ocean Oscillation), Arabian Sea and Bay of Bengal could be linked with the rainfall and temperature conditions of the coastal belts. Overall, negative association between rainfall and T_{max} also displays a similar spatial distribution pattern as that of annual cross correlation.

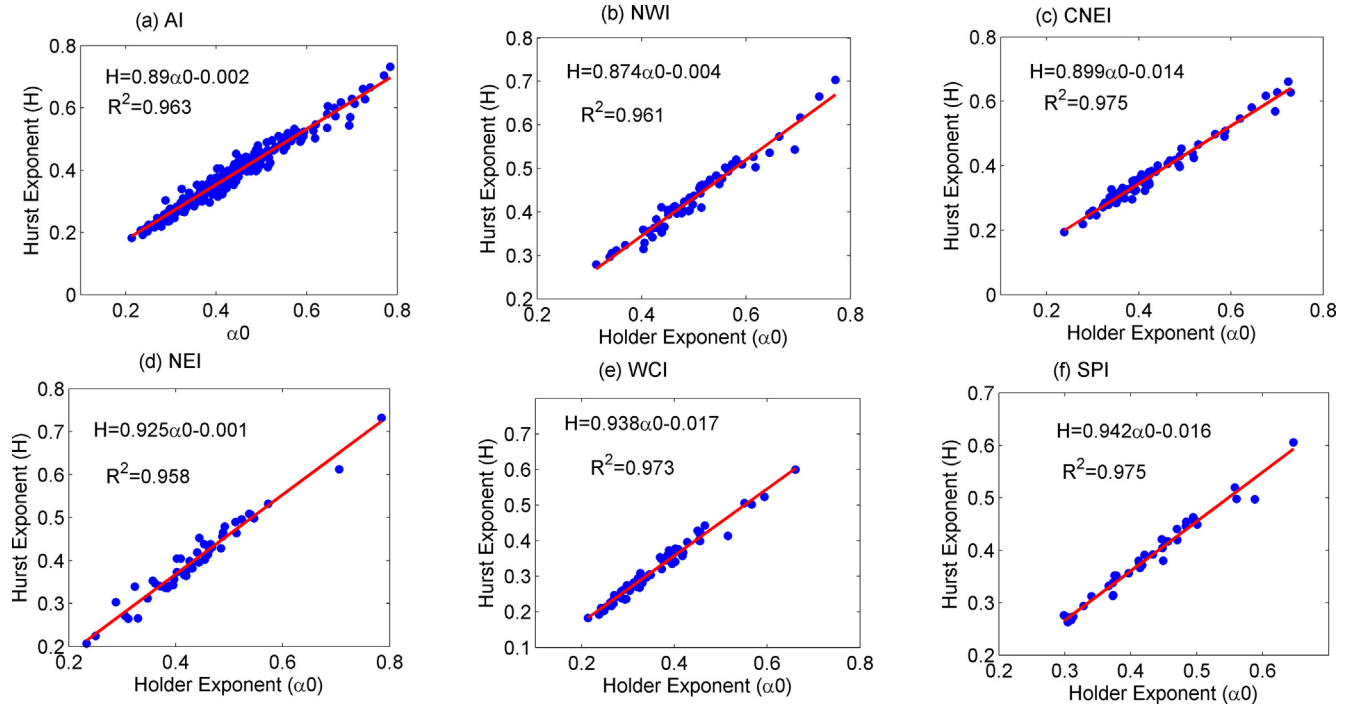

Fig. 7. Relation between Hurst Exponent and Holder exponent in different macro regions in India (a) AI; (b) NWI (c) CNEI 9d) NEI (e) WCI (f) SPI.

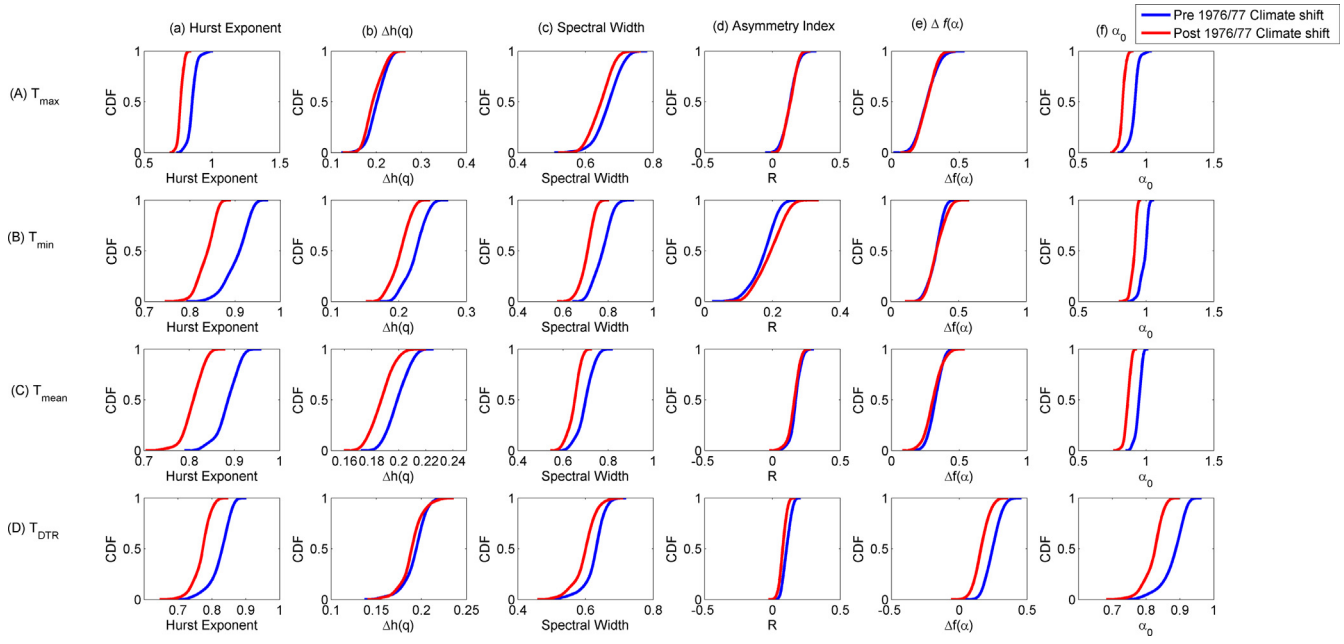

Fig. 8. PDFs and CDFs of multifractal properties of four temperature time series for pre and post 1977 Pacific climatic shift (a) Hurst exponent; (b) spread of generalized Hurst exponent (Δh(q)); spectral width; (d) asymmetry index (R); (e) spread of singularity spectrum (Δf(α)); (f) Holder exponent (α0).

According to Fig. 10, it is evident that strong persistence of mean temperature exists in most of the regions and among which the strongest persistence is displayed at the coastal belts and Peninsular India, while the weakest persistence exists in the NWI. In this case also for all grid points, the joint persistence lies between that of rainfall and T_{mean} time series. The seasonal cross correlation is negative at all regions except some parts of Peninsular India and upper Himalaya. At annual scale, relatively higher correlations are noted in the T_{mean} - rainfall link when compared with the T_{max} - rainfall link (positive correlation up to 0.78). In this case also, the strong positive correlations are clustered in the Peninsular India and the coastal belts, while negative association is noted only in the NWI and few localized grids of WCI. Again, the spatial distribution of overall correlation is identical to that of annual correlation except with a lesser magnitude in the correlations.

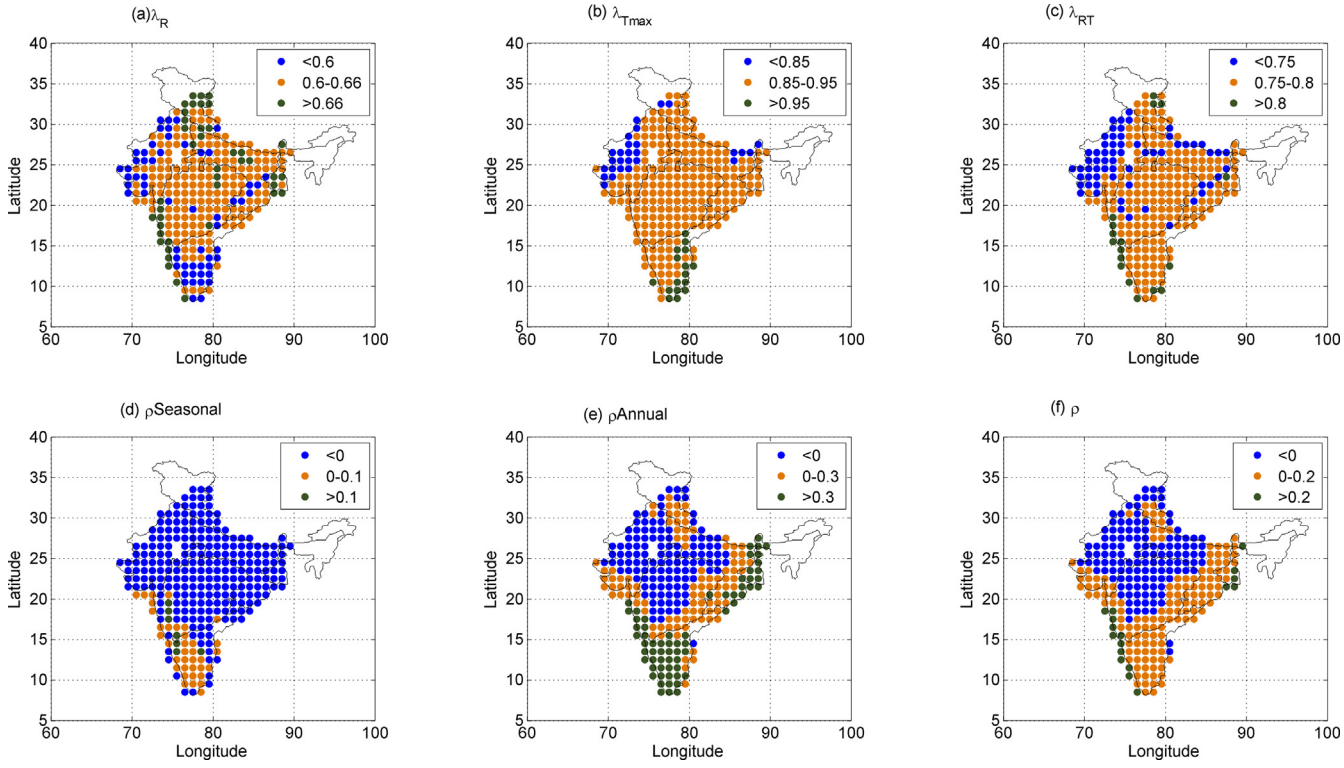

Fig. 9. Spatial distributions of scaling exponent and cross correlation values of rainfall and T_{max} time series. λ_R and λ_{Tmax} denote the individual persistence of rainfall and maximum temperature time series, whereas λ_{RT} denotes the joint persistence of rainfall and temperature. ρSeasonal and ρAnnual are the correlation coefficients at seasonal and annual scales and ρ denotes the overall correlation between temperature and rainfall time series.

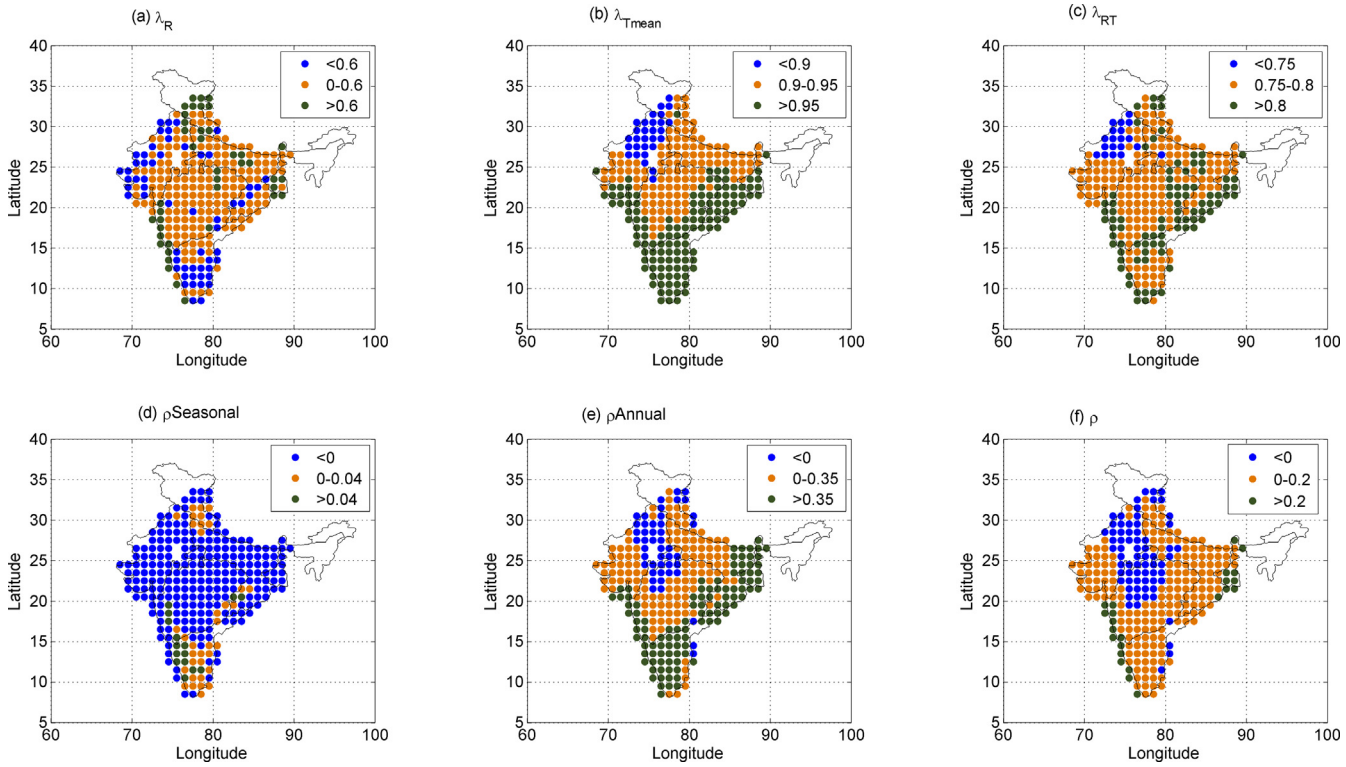

Fig. 10. Spatial distributions of scaling exponents and cross correlation parameters of rainfall and T_{mean} time series. λ_R and λ_{Tmean} denote the individual persistence of rainfall and maximum temperature time series, whereas λ_{RT} denotes the joint persistence of rainfall and temperature. ρSeasonal and ρAnnual are the correlation coefficients at seasonal and annual scales and ρ denote the overall correlation between temperature and rainfall time series.

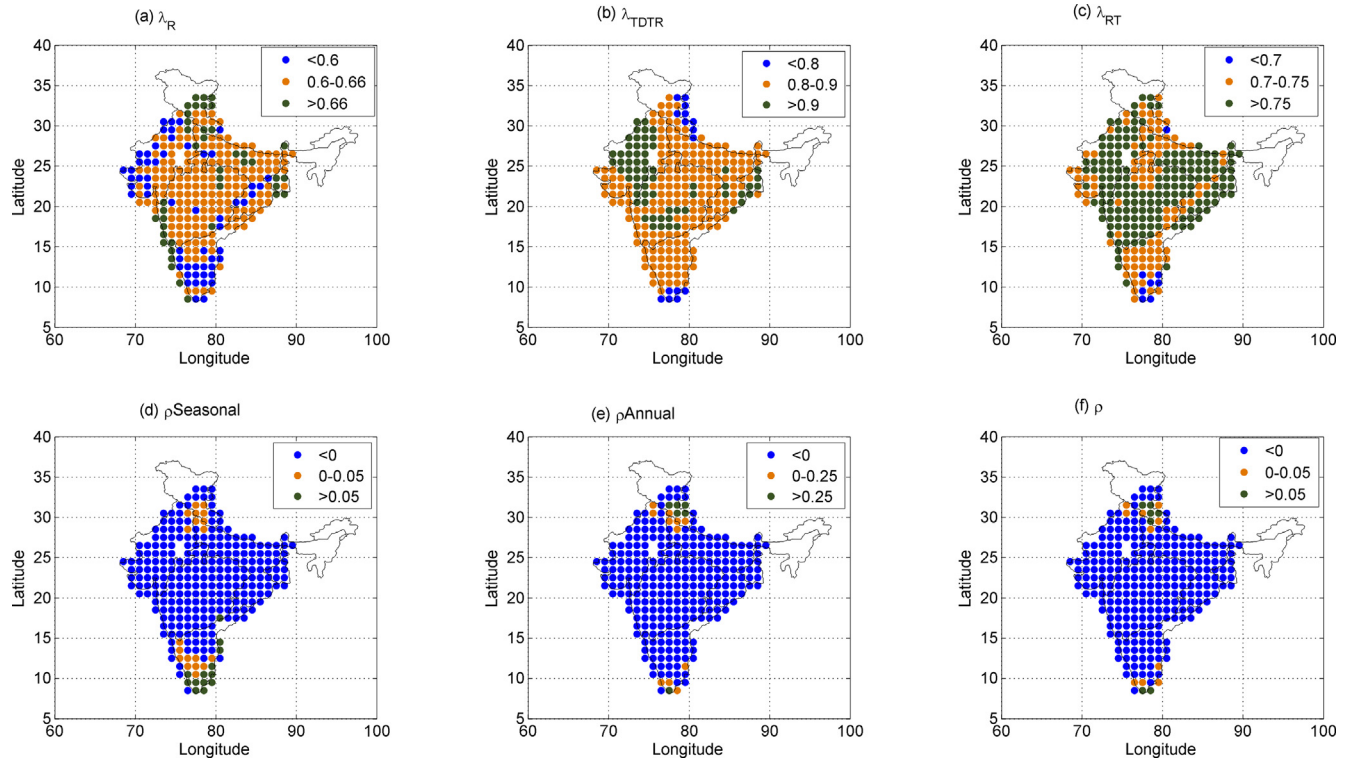

Fig. 11. Spatial distributions of scaling exponents and cross correlation parameters of rainfall and T_{DTR} time series. λ_R and λ_{TDTR} denote the individual persistence of rainfall and maximum temperature time series, whereas λ_{RT} denotes the joint persistence of rainfall and temperature. ρSeasonal and ρAnnual are the correlation coefficients at seasonal and annual scales and ρ denotes the overall correlation between temperature and rainfall time series.

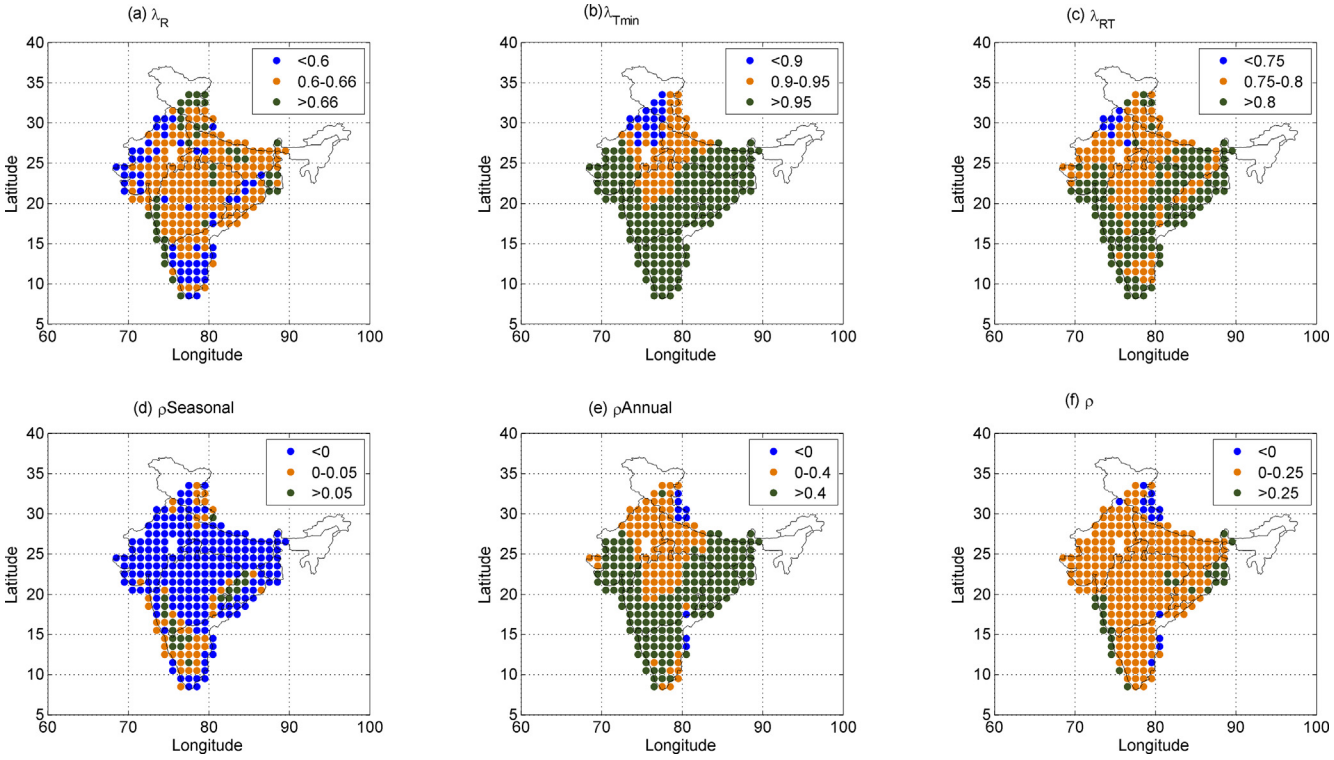

Fig. 12. Spatial distributions of scaling exponents and cross correlation parameters of rainfall and T_{min} time series. λ_R and λ_{Tmin} denote the individual persistence of rainfall and maximum temperature series, whereas λ_{RT} denotes the joint persistence of rainfall and temperature. ρSeasonal and ρAnnual are the correlation coefficients at seasonal and annual scales and ρ denotes the overall correlation between temperature and rainfall time series.

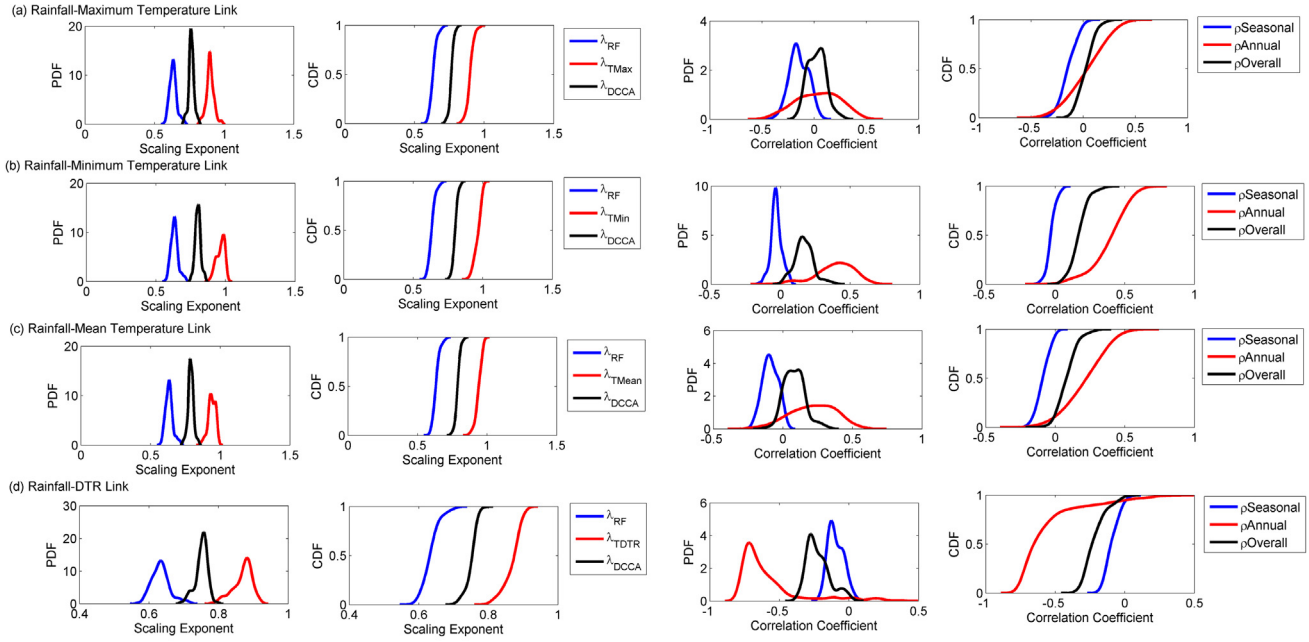

Fig. 13. PDFs and CDFs of seasonal correlation, annual correlation and overall correlation of (a) rainfall-maximum temperature link; (b) rainfall-minimum temperature link; (c)rainfall-mean temperature link; (d) rainfall-DTR link.

From Fig. 11 it is noted that for the DTR time series, the strongest persistence is in the North West India. In the spatial distribution of joint persistence, the WCI and CNEI (the eastern coast in particular) display the highest persistence along with the NWI region. The seasonal correlation and overall correlation are found to be negative except in the Western Himalayan and southern Peninsular regions. At annual scale also, the positive correlation is noted only in these regions. The temperature difference has distinctly different influence on the rainfall pattern when compared with other temperature time series.

The association between minimum temperature and rainfall is unique when compared with other links. The strongest persistence property is noticed for the T_{min} time series (minimum of 0.849 to maximum of 0.997 with a mean of 0.971) when compared with other three temperature time series. The seasonal correlation is negative in the NWI

and majority of the parts of NCI and CNEI. There is a clear switchover in the nature and strength of association in the T_{min}-rainfall link at annual scale. It is also noted that some geographical regions of India, the correlation changes from negative (at seasonal scale) to positive (even $>$ 0.5 at annual scale). The Peninsular region and coastal belts of India display the highest persistence property, the influence of which is reflected also in the mean temperature time series (see Fig. 10). Peninsular region of India is bounded by the Bay of Bengal in the east, Indian Ocean in the south and Arabian sea in the west. This oceanic proximity plays a dominant role in the precipitation of the country, which is influenced by the temperature anomalies and local surface warming. Global and regional temperature and precipitation variability is influenced by ENSO phenomenon (Davey et al., 2014). Also, it is well proven that other large scale atmospheric circulations such as Quasi Biennial Oscillation (QBO), Equatorial Indian Ocean Oscillation (EQUINOO), North Atlantic Oscillation (NAO), Atlantic Multi Decadal Oscillation (AMO) etc. are all playing major roles on seasonal rainfall. The co-existence of multiple oscillations also may modulate the process (Gadgil et al., 2004) and one cannot separate the rainfall and near surface temperature states in India. It is hard to find a universal pattern such as how the scaling exponents change with latitude, altitude or distance from the coast (Yu et al., 2014). Also attributing the reason for multifractality to single indicator is quite impossible as the Indian monsoon system is quite complex and many local processes and details like moisture, terrain, vegetation effects may influence the regional precipitation variations. The PDFs and CDFs of DCCA parameters of rainfall and four temperature time series links are presented in Fig. 13.

Considering the T_{max}- rainfall link, the mean values are 0.63 and 0.87 respectively for rainfall and T_{max} time series and the joint persistence lies between that of individual persistence (with a mean of 0.76). For 234 grid points, the seasonal correlation is negative and for 119 points, annual correlation is negative. It is found that almost 39% of ρAnnual values lay between -0.2 and 0.2. Also 35% of ρAnnual values lay between 0.2 and 0.6 and remaining 26% of ρAnnual values lay between -0.6 and -0.2. Except for 69 points, the annual correlation is more than that of seasonal correlation while the overall correlation is positive for 150 points. The relative magnitude of persistence of the rainfall, T_{max} and joint persistence is clear from Fig. 11 and follows the universal property in their relative magnitudes (Hajian and Movahed 2010). The scaling exponent of mean temperature varies between 0.83 and 0.99. The persistence of rainfall time series found to be less than that of temperature in all grid points (with a mean of 0.63 and 0.95, respectively) while the joint persistence is nearly half of individual persistence values (with a mean of 0.78). In 79% the grid points (227 out of 286), the correlation is negative at seasonal scale while the correlation is positive at annual scale for 231 grid points (80.8% of grids). Except for 31 grid points, annual correlation is greater than that of seasonal correlation. Also it is noted that for 55% of grids ρAnnual lies between 0 and 0.4 and for 15% grids, the correlation lies between 0.4 and 0.8. For 208 grid points, the overall correlation between rainfall and T_{mean} is weakly positive and the overall mean correlation is found to be around 0.08.

In the T_{DTR}-rainfall link, it was found that the mean scaling exponent of temperature time series is around 0.87 and the mean value of joint persistence was found to be 0.75. In this case also, for all grid points the joint persistence is between those of individual persistence of rainfall and temperature. Except for 17 grid points, the overall correlation is negative with a mean of -0.237. Similar response is noted for annual and seasonal correlations. i.e., for 260 and 240 grid points, the rainfall-temperature association is negative at these time scales. But annual correlation is strongly negative (with overall mean of -0.89) while seasonal correlation is weakly negative (with overall mean of -0.27). At annual time scale, the positive correlation varies up to 0.49, while at seasonal scale, it varies only up to 0.11. The scaling exponent of minimum temperature varies between 0.85 and 0.99 with a mean of 0.97, which infers very strong persistence. The joint persistence clearly lies between the individual persistence, with a mean scaling exponent of 0.8. Interestingly, the seasonal correlation was found to be negative in 210 grid points (73.4% of grid points) with an overall mean value of -0.192, but at annual scale, the correlation was strongly positive in 268 grid points (out of 294). The mean correlation value is 0.426 (with minimum of -0.21 and maximum of 0.8). This is a clear evidence of change in the scale dependent nature of association in the minimum temperature- rainfall link. In this case, the overall correlation was also found to be positive in 263 grid points with a mean value of 0.156 (varies between -0.05 and 0.46).

5. Discussion on applications and future scope

This study examined the multifractal properties of daily rainfall field over India to get an insight into the complexity and persistence properties of the variable. The spatio-temporal variability of the multifractal properties adduced some interesting judgments and possible reasons for their diversity. Ascertaining the role of persistence is vital to the development of hydro-meteorological studies and the changes in the persistence over the time spell should be investigated. Any significant change in the persistence may lead to erroneous predictions and the situation is quite analogous to the use of a stationarity assumption under a non-stationary environment in a changing climate scenario. The high degree of complexity and multifractality of rainfall in regions like NWI demands the multifractal modeling in such areas for specific applications. The predictability could be well assessed by the persistence and the predictions in regions like NEI this information could have an added value in devising new paradigms for accurate modeling of rainfall. The temporal change in the properties of rainfall with respect to the pacific climatic shift is not supporting the urgent need of non-stationary modeling in the country as a whole, even though a reduction in complexity and multifractality along with an increase in persistence is noted in majority of the grid points. However, localized analysis using station-wise data may give improved understanding on the modeling practices to be followed for the management of the water resources. The rainfall-temperature cross-correlation studies in a multiscale-multifractal framework provided remarkable insights in the behavior of rainfall in Indian subcontinent. The nature of association of each temperature time series with rainfall in India is quite different from that of the other. Despite these differences, the persistence and correlation properties of the dataset of Peninsular India and Coastal belts show distinctly different behavior than the rest parts of the country. More emphasis should be given on multifractal and non-stationary frameworks for modeling hydrological variables in these regions, which may eventually help in accurate management of the water resources.

Understanding the multifractal properties of rainfall time series may help for multifractal modeling, simulation and synthetic generation of rainfall fields, de-noising etc. (Deidda et al. 1999; Deidda 1999, 2000; Serinaldi 2010), which are some promising domains for subsequent researches. The scaling exponents can be used for derivation of Intensity-Duration-Frequency curves by rainfall disaggregation (Veneziano and Furcolo 2002; Huang et al. 2014; Garcia-Marin et al., 2019). The space–time disaggregation of rainfall is a possible application for the scaling exponents developed (Deidda 2000; Hubert 2001; Pathirana et al. 2007). Potential applicability of decomposition methods such as wavelet transforms can be conjunctively used along with multifractal properties in the space–time disaggregation studies (Nourani et al., 2013, 2017; Roushangar et al. 2019). The derived multifractal properties may help in performing the catchment classification or regionalization and subsequent predictions in ungauged basins, by coupling with different clustering techniques (Sharghi et al., 2018; Baghanam et al., 2019). To get a more comprehensive picture of the multifractal properties of rainfall fields, similar studies can be performed using more fine resolution data (say 0.25°x0.25°) and cross correlations with other hydrological variables (like station-wise

streamflow) can be analyzed in a multifractal perspective. This study provided an overall picture of multifractal characteristics of the rainfall and temperature datasets in India. In-depth studies using the real field datasets are highly recommended, in coastal and peninsular India in particular. While accepting the constraints on rainfall time series of longer stretch, it is always advisable to perform similar studies using the real-time datasets.

6. Conclusions

In this study, the multifractality of 1^{o}x1^{o} daily gridded rainfall fields over India was evaluated using MF-DFA method and its link with the four different temperature datasets was investigated using the MF-DCCA method. The daily gridded rainfall data of 87% grid points possessed short term persistence and most of the time series showed strong multifractal behavior. The highest multifractal degree and persistence was noted in the NWI followed by NEI, where the rainfall pattern is more homogeneous in characteristics. There is a clear reduction in multifractal degree of rainfall time series of India for the post 1976/77 Pacific climatic shift period. The joint persistence of rainfall and temperature was nearly half of the persistence of individual time series in all of the combinations of rainfall-temperature linkages. The nature and strength of cross correlation between temperature and rainfall displayed spatio-temporal diversity. The correlation properties between rainfall and temperature were unique in the Peninsular and coastal belts of India, when compared to other regions, which could be attributed to the effect of large scale climatic circulations resulting from oceanic proximity.

CRediT authorship contribution statement

S. Adarsh: Project administration, Methodology. **Vahid Nourani:** Conceptualization, Supervision, Methodology, Writing - review & editing. **D.S. Archana:** Investigation, Resources, Data curation. **Drisya S. Dharan:** Formal analysis, Writing - original draft.

Declaration of Competing Interest

The authors declare that they have no known competing financial interests or personal relationships that could have appeared to influence the work reported in this paper.

Acknowledgement

The authors acknowledge the service of India Meteorological Department (IMD) for providing the 1^{o}x1^{o} daily rainfall and temperature time series for performing this research work at TKM College of Engineering Kollam, India.

References

Adarsh, S., Nagesh Kumar, D., Deepthi, B., Gayathri, G., Aswathy, S.S., Bhagyasree, S., 2019. Multifractal characterization of meteorological drought in India using detrended fluctuation analysis. Int. J. Climatol. 39 (11), 4234–4255.

Adarsh, S., Dharan, D.S., Anuja, P.K., Aggie Suman 2018. Unravelling the scaling characteristics of daily streamflows of Brahmani river basin, India using Arbitrary Order Hilbert Spectral and Detrended Fluctuation Analyses. SN Applied Sciences, DOI: 10.1007/s42452-018-0056-1.

Adarsh, S., Janga, Reddy M., 2016. Analysing the hydroclimatic teleconnections of summer monsoon rainfall in Kerala, India using Multivariate Empirical Mode Decomposition and time dependent intrinsic Correlation. IEEE Geosci. Remote Sens. Lett. 13 (9), 1221–1225.

Baghanam, A.H., Nourani, V., Keynejad, M.A., Taghipour, H., 2019. Conjunction of wavelet-entropy and SOM clustering for multi-GCM statistical downscaling. Hydrol. Res. 50 (1), 1–23.

Brito, A.A., Santos, F.R., de Castro, A.P.N., da Cunha Lima, A.T., Zebende, G.F., da Cunha Lima, I.C., 2018. Cross-correlation in a turbulent flow: Analysis of the velocity field using the σ DCCA coefficient. EPL (Europhysics Letters) 123 (2), 20011.

Burgueño, A., Lana, X., Serra, C., Martínez, M.D., 2014. Daily extreme temperature multifractals in Catalonia (NESpain). Phys. Lett. A 378 (2014), 874–885.

Cadenas, E., Campos- Amezcua, R., Rivera, W., Espinosa-Medina, M.A., Méndez-Gordillo, A.R., Rangel, E., Tena, J., 2019. Wind speed variability study based on the Hurst coefficient and fractal dimensional analysis. Energy Sci. Eng. 7, 361–378.

Dahlstedt, K., Jensen, H., 2005. Fluctuation spectrum and size scaling of river flow and level. Phys. A 348, 596–610.

Davey, M.K., Brookshaw, A., Ineson, S., 2014. The probability of the impact of ENSO on precipitation and near-surface temperature. Clim. Risk Manage. 1, 5–24.

Dey, P., Mujumdar, P.P., 2018. Multiscale evolution of persistence of rainfall and streamflow. Adv. Water Resour. 121, 285–303.

Deidda, R., Benzi, R., Siccardi, F., 1999. Multifractal modeling of anomalous scaling laws in rainfall. Water Resour. Res. 35 (6), 1853–1867.

Deidda, R., 1999. Multifractal analysis and simulation of rainfall fields in space. Physics and Chemistry of Earth: Part B. 24 (1–2), 73–78.

Deidda, R., 2000. Rainfall downscaling in a space-time multifractal framework. Water Resour. Res. 36 (7), 1779–1794.

Drożdż, S., Minati, L., Oświecimka, P., Stanuszek, M., Wątorek M., 2019. Signatures of the Crypto-Currency Market Decoupling from the Forex. Future Internet 11, 154. https://doi.org/10.3390/fi11070154.

Drożdż, S., Oświecimka, P, 2015. Detecting and interpreting distortions in hierarchical organization of complex time-series. Phys. Rev. E 91, 030902.

Gadgil, S., Vinayachandran, P.N., Francis, P.A., Gadgil, S., 2004. Extremes of the Indian summer monsoon rainfall, ENSO and equatorial Indian Ocean oscillation. Geophys. Res. Lett. 31, L12213. https://doi.org/10.1029/2004GL019733.

Garcia-Marin, A.P., Morbidelli, R., Saltalippi, C., Cifrodelli, M., Esteveza, J., Flammini, A., 2019. On the choice of the optimal frequency analysis of annual extreme rainfall by multifractal approach. J. Hydrol. 575 (2019), 1267–1279.

Hajian, S., Movahed, M.S., 2010. Multifractal detrended cross-correlation analysis of sunspot numbers and river flow fluctuations. Phys. A 389 (2010), 4942–4954.

Hou, W., Feng, G., Yan, P., Li, S., 2018. Multifractal analysis of the drought area in seven large regions of China from 1961 to 2012. Meteorol. Atmos. Phys. 130, 459–471.

Huang, Y., Schmitt, F.G., Lu, Z., Liu, Y., 2009. Analysis of daily river flow fluctuations using empirical mode decomposition and arbitrary order Hilbert spectral analysis. J. Hydrol. 373, 103–111.

Huang, Q., Chen, Y., Xu, S., Liu, J., 2014. Case study of applying Multifractal models for rainfall IDF analysis in China. J. Hydrol. Eng. 19 (1). https://doi.org/10.1061/(ASCE)HE.1943-5584.0000781.

Hubert, P., 2001. Multifractals as a tool to overcome scale problems in hydrology. Hydrol. Sci. J. 46 (6), 897–905.

Hurst, H.E., 1965. Long-term storage : An experimental study. Constable, London.

Ihlen, E.A.F.E., 2012. Introduction to multifractal detrended fluctuation analysis in MATLAB. Front. Physiol. 3, 141.

Kantelhardt, J.W., Rybski, D., Zschiegner, S.A., Braun, P., Koscielny-Bunde, E., Livina, V., Havlin, S., Bunde, A., 2003. Multifractality of river runoff and precipitation: comparison of fluctuation analysis and wavelet methods. Phys. A 330, 240–245.

Kantelhardt, J.W., Koscielny-Bunde, E., Rybski, D., Braun, P., Bunde, A., Havlin, S., 2006. Long-term persistence and multifractality of precipitation and river runoff records. Journal of Geophysical Research: Atmospheres 111 (D1).

Kantelhardt, J.W., Zschiegner, S.A., Koscielny-Bunde, E., Havlin, S., Bunde, A., Stanley, H.E., 2002. Multifractaldetrended fluctuation analysis of nonstationary time series. Phys. A 316 (1–4), 87–114.

Karatasou, S., Santamouris, M., 2018. Multifractal analysis of high-frequency temperature time series in the urban environment. Climate 6 (2), 50.

Krzyszczak, J., Baranowski, P., Zubik, M., Kazandjiev, V., Georgieva, V., Sławiński, C., Siwek, K., Kozyra, J., Nieróbca, A., 2018. Multifractal characterization and comparison of meteorological time series from two climatic zones. Theor. Appl. Climatol. https://doi.org/10.1007/s00704-018-2705-0.

Kwapień, J., Oświęcimka, P., Drożdż, S., 2015. Detrended fluctuation analysis made flexible to detect range of cross-correlated fluctuations. Phys. Rev. E 92 (5), 052815.

Li, E., Mu, X., Zhao, G., Gao, P., 2015. Multifractal detrended fluctuation analysis of streamflow in the Yellow River Basin. China. *Water* 7 (4), 1670–1686.

Miller, A.J., Rayan, D.R., Barnett, T.P., Graham, N.E., Oberhuber, J.M., 1994. The 1976–77 Climate Shift of the Pacific Ocean. Oceanography 7 (1), 21–26.

Mandelbrot, B., 1982. The fractal geometry of nature. WH Freeman Publishers, New York.

Nourani, V., Andalib, G., Dąbrowska, D., 2017. Conjunction of wavelet transform and SOM-mutual information data pre-processing approach for AI-based Multi-Station nitrate modeling of watersheds. J. Hydrol. 548, 170–183.

Nourani, V., Baghanam, A.H., Adamowski, J., Gebremichael, M., 2013. Using self-organizing maps and wavelet transforms for space–time pre-processing of satellite precipitation and runoff data in neural network based rainfall–runoff modeling. J. Hydrol. 476, 228–243.

Roushangar, K., Nourani, V., Alizadeh, F., 2019. A multiscale time-space approach to analyze and categorize the precipitation fluctuation based on the wavelet transform and information theory concept. Hydrol. Res. 49 (3), 724–743.

Olsson, J., Niemczynowicz, J., 1996. Multifractal analysis of daily spatial rainfall distributions. J. Hydrol. 187 (1–2), 29–43.

Oświecimka, P., Drożdż, S., Forczek, M., Jadach, S., Kwapień, J, 2014. Detrended cross-correlation analysis consistently extended to multifractality. Phys. Rev. E 89 (2), 023305.

Pandey, G., Lovejoy, S., Schertzer, D., 1998. Multifractal analysis of daily river flows including extremes for basins five to two million square kilometers, one day to 75 years. J. Hydrol. 208, 62–81.

Pathirana, P., Herath, S., Yamada, T., 2007. Estimating rainfall distributions at high temporal resolutions using a multifractal model. Hydrology and Earth System Science 7 (5), 668–679.

Peng, C.K., Buldyrev, S.V., Havlin, S., Simons, M., Stanley, H.E., Goldberger, A.L., 1994. Mosaic organization of DNA nucleotides. Phys. Rev. E 49 (2), 1685.

Piao, L., Fu, Z., 2016. Quantifying distinct associations on different temporal scales: comparison of DCCA and Pearson methods. *Sci. Rep.* 6, 36759.
Podobnik, B., Stanley, H.E., 2008. Detrended cross-correlation analysis: a new method for analyzing two nonstationary time series. Phys. Rev. Lett. 100 (8), 084102.
Ross, R.S., Krishnamurti, T.N., Pattnaik, S., Pai, D.S., 2018. Decadal surface temperature trends in India based on a new high resolution data set. Sci. Rep. 8, 7452. https://doi.org/10.1038/s41598-018-25347-2 (2018).
Sahana, A.S., Ghosh, S., Ganguly, A., Murtugudde, R., 2015. Shift in Indian summer monsoon onset during 1976/1977. Environ. Res. Lett. 10 (2015), 054006.
Serinaldi, F., 2010. Multifractality, imperfect scaling and hydrological properties of rainfall time series simulated by continuous universal multifractal and discrete random cascade models. Nonlinear Processes Geophys. 17 (6), 697–714.
Sharghi, E., Nourani, V., Soleimani, S., Sadikoglu, F., 2018. Application of different clustering approaches to hydroclimatological catchment regionalization in mountainous regions, a case study in Utah State. J. Mountain Sci. 15 (3), 461–484.
Tan, X., Gan, T.W., 2017. Multifractality of Canadian precipitation and streamflow. Int. J. Climatol. 37 (S1), 1221–1236.
Tessier, Y., Lovejoy, S., Hubert, P., Schertzer, D., Pecknold, S., 1996. Multifractal analysis and modeling of rainfall and river flows and scaling, causal transfer functions. J. Geophys. Res. 101, 26427–26440.
Vassoler, R.T., Zebende, G.F., 2012. DCCA cross-correlation coefficient apply in time series of air temperature and air relative humidity. Phys. A 391 (7), 2438–2443.
Veneziano, A., Furcolo, P., 2002. Multifractality of rainfall and scaling of intensity-duration-frequency curves. Water Resour. Res. 38 (12), 1–12.
Vinnarasi, R., Dhanya, C.T., Chakravorthy, A., Aghakouchak, A., 2017. Unravelling diurnal asymmetry of surface temperature in different climate zones. *Sci. Rep.*, Nature Publishing Group,. https://doi.org/10.1038/s41598-017-07627-5. (2017).
Wang, X., Mei, Y., Li, W., Kong, Y., Cong, X., 2016. Influence of sub-daily variation on Multifractal Detrended Fluctuation Analysis of wind speed time series. PLoS ONE 11 (1), e0146284. https://doi.org/10.1371/journal.pone.0146284.
Wu, Y., He, Y., Wu, M., Lu, C., Gao, S., Xu, Y., 2018. Multifractality and cross-correlation analysis of streamflow and sediment fluctuation at the apex of the Pearl River Delta. Sci. Rep. 8 (1), 16553.
Yu, Z.G., Leung, Y., Chen, Y.D., Zhang, Q., Anh, V., Zhou, Y., 2014. Multifractal analyses of daily rainfall time series in Pearl River basin of China. Phys. A 405, 193–202.
Zebende, G.F., 2011. DCCA cross-correlation coefficient: Quantifying level of cross-correlation. Phys. A 390 (4), 614–618.
Zhou, W.-X., 2008. Multifractal detrended cross-correlation analysis for two non-stationary signals. Phys. Rev. E 77, 066211. https://doi.org/10.1103/PhysRevE.77.066211.